Hindawi
Advances in Materials Science and Engineering
Volume 2020, Article ID 7365862, 10 pages
https://doi.org/10.1155/2020/7365862

Research Article

Effect of Nano-$CaCO_3$ on the Mechanical Properties and Durability of Concrete Incorporating Fly Ash

Yanqun Sun, Peng Zhang, Weina Guo, Jiuwen Bao, and Chengping Qu

School of Civil Engineering, Qingdao University of Technology, Qingdao 266033, China

Correspondence should be addressed to Peng Zhang; peng.zhang@qut.edu.cn

Received 18 January 2020; Accepted 23 March 2020; Published 9 April 2020

Academic Editor: Ivan Giorgio

Concrete mixtures consisting of nanomaterials and fly ash have been shown to be effective for improving the performance of concrete. This study investigates the combined effects of nano-$CaCO_3$ and fly ash on the mechanical properties and durability of concrete; the mix proportion is optimized through orthogonal experiments. In the first phase, nine concrete mixtures were prepared with three water-to-binder ratios (0.4, 0.5, and 0.6), three fly ash contents (15%, 20%, and 25% replacement of the cement weight), and three nano-$CaCO_3$ contents (1%, 2%, and 3% replacement of the cement weight). Based on the orthogonal analysis, the optimal concrete mix proportion was determined as a water-to-binder ratio of 0.4, 20% fly ash, and 1% nano-$CaCO_3$. In the second phase, further investigations were carried out to examine the superiority of the optimal concrete and evaluate the synergistic effect of nano-$CaCO_3$ and fly ash. The results showed that nano-$CaCO_3$ contributed to increasing the compressive strength of fly ash concrete at the early ages, but its effect was quite limited at later ages. Furthermore, the scanning electron microscopy analysis revealed that the seeding effect, filling effect, and pozzolanic effect were the primary mechanisms for the improvement of concrete performance.

1. Introduction

In recent years, concrete has been used extensively for the construction of high-rise buildings and marine structures as well as for long-span bridges under harsh environmental conditions [1]. To satisfy the demands of these applications, modern concrete materials must possess high strength, toughness, and durability. However, concrete has some intrinsic defects, such as low tensile strength, poor toughness, and high brittleness, which makes it susceptible to deterioration under adverse conditions [2]. As a by-product of industrial processes, the addition of fly ash to concrete not only benefits the environment but also confers economic benefits [3]. Moreover, fly ash possesses pozzolanic activity that reacts with calcium hydroxide (CH) during cement hydration, forming additional hydration products such as calcium silicate hydrate (C-S-H) and calcium aluminate hydrate (C-A-H) [4]. Most previous studies [5–10] have shown that these hydration products of the pozzolanic reaction can effectively improve the density of concrete, leading to higher strength and better durability. For instance, the resulting reduced permeability of concrete can inhibit damage to the concrete through the alkali–aggregate reaction. However, the pozzolanic reaction of fly ash is slow, with lower strength at early ages, which remains a concern.

Recently, valuable research has been conducted to investigate the influence of nanomaterials on the properties of concrete. Jo et al. [11] reported that nano-SiO_2 can improve the compressive and flexural strength of cement mortars. Nazari et al. [12] showed that the hydration degree of cement was also improved with the addition of nano-Al_2O_3. Meanwhile, Senff et al. [13] and Nazari et al. [14] found that the setting time of fresh cement paste could be shortened by nano-SiO_2 and nano-Al_2O_3, and the initial setting time and the final setting time became shorter with the increase of the nanoparticles content. Thus, combining nanomaterials with fly ash could provide a more practical and reliable method for enhancing the properties of concrete. However, it is undeniable that their high cost restricts the application and development of nanomaterials [15]. Moreover, it must be

taken into consideration that nanomaterials may be difficult to disperse in the cement paste owing to their huge specific surface area and strong surface activity [16].

Owing to its high efficacy and inexpensive price, nano-$CaCO_3$ has been widely used in the plastics industry as an additive [17]. If nano-$CaCO_3$ has a positive effect when added to concrete, it could be a feasible prospect for the application of nanomodified concrete. Chemically, nano-$CaCO_3$ can improve the rate of reaction of tricalcium aluminate (C_3A) to form a carboaluminate complex, increasing the total hydration products and thus the strength [18]. In addition, it also reacts with tricalcium silicate (C_3S) and promotes setting, producing a higher volume of hydrates, which are effective for filling the microstructure [19]. As a consequence, nano-$CaCO_3$ concrete possesses a higher initial strength [20, 21]. Sato and Diallo [22] studied the influence of nano-$CaCO_3$ on cement hydration, and the results revealed that the rapid growth of C-S-H was significantly improved by adding nano-$CaCO_3$ owing to the seeding effect of the nanoparticles. Supit and Shaikh [23] evaluated four different contents of nano-$CaCO_3$ added to fly ash concrete, and the results showed that the addition of 1% nano-$CaCO_3$ provided an optimal improvement in the compressive strength of concrete. Xu et al. [24] reported that the addition of 1%-2% nano-$CaCO_3$ could improve the compressive strength of high-performance concrete by 13%–18%.

While most studies have investigated the effects of nano-$CaCO_3$ and fly ash on the hydration, compressive strength, and microstructure of concrete, only a few have performed detailed investigations of the comprehensive performance of concrete containing nano-$CaCO_3$ and fly ash. Therefore, the objectives of this study were to investigate the synergistic mechanism for the effect of nano-$CaCO_3$ and fly ash not only on strength development but also on the durability of concrete, including its chloride penetrability, carbonation resistance, and frost resistance. In addition, the optimal concrete mix proportion was determined. The results of this study may serve to facilitate the proper use of nano-$CaCO_3$ and fly ash in concrete to achieve the increasing demands of practical applications.

2. Materials and Methods

2.1. Materials. Ordinary Portland cement with a 28-d compressive strength of 42.5 MPa and class I fly ash with a surface area of approximately 380 m^2/kg were used as cement paste materials. The chemical compositions of the ordinary Portland cement and fly ash are listed in Table 1. River sand with a maximum particle size of 5 mm and granite gravel with a particle size range of 5 mm to 20 mm, both from the Qingdao area, were used as the fine aggregate and coarse aggregate, respectively. Nano-$CaCO_3$ was used in this study owing to its lower price, and the physical properties of nano-$CaCO_3$ are summarized in Table 2. One type of polycarboxylate superplasticizer was used as an additive to the concrete to obtain the desired slump and fluidity as well as to act as a dispersant for the nano-$CaCO_3$.

2.2. Test Specimens. In the first phase, a total of 90 concrete cubes with a size of 100 mm were produced for compressive strength tests, and 30 prism specimens with dimensions of 100 mm × 100 mm × 400 mm were produced for flexural strength tests. In the second phase, the 100 mm concrete cube specimens, 100 mm × 100 mm × 400 mm prism specimens, and cylindrical specimens with dimensions of 100 mm × 50 mm were cast for tests of mechanical properties and durability. All of the specimens were demolded after one day and placed under a standard condition ($T = 20 \pm 2^{\circ}C$ and RH ≥ 95%) to cure until the testing ages. A set of three specimens were tested for each concrete mix, and the average value was reported as the final value. The reference concrete mix contained 190 kg/m^3 water, 380 kg/m^3 cement, 622 kg/m^3 fine aggregate, and 1208 kg/m^3 coarse aggregate; the weight of water reducer was adjusted according to the nano-$CaCO_3$ content. For all mixes, the weights of water and aggregate were kept constant. It should be noted that nano-$CaCO_3$ is insoluble in water. However, polycarboxylate superplasticizer has a strong dispersing effect; and therefore nano-$CaCO_3$ could be dispersed in water and form a substantially uniform mixed solution with a high-speed mixing. Half of the solution was then mixed with cement and aggregates for 30 s. After that, another half of the solution was added to the mixtures, followed by further stirring for 90 s.

2.3. Orthogonal Experiments. The orthogonal experiments were designed based on statistics; the test data was analyzed using mathematical methods, and the factors and levels were simplified to obtain the optimal mix proportion [25]. Three factors affecting the properties of concrete were studied: (A) the water-to-binder ratio (W/C), (B) the fly ash content, and (C) the nano-$CaCO_3$ content. Each factor was designed with three different levels (https://www.sciencedirect.com/science/article/pii/S095006181932478X?via=ihub, Table 3). According to the L9 (3^4) orthogonal experiment design table, a total of ten concrete mixtures were tested, including one reference concrete (https://www.sciencedirect.com/science/article/pii/S095006181932478X?via=ihub, Table 4). The tests of mechanical properties were conducted based on standard GB/T50081-2002 [26]. At ages of 3, 7, and 28 d, the cubic specimens were removed from the curing room for compressive strength tests. After 28 d of aging, the flexural strength of the prism specimens was measured using the third-point loading method. The test levels and compositions of the concrete specimens were selected based on previous studies [27, 28].

A range analysis was conducted to determine the order of influence and select the optimal level of each factor. Based on the range analysis, the values of K and R were first calculated. The K value for each level of a parameter is the sum of three values of samples with the same level, and the highest K value represents the optimal level. The R value is an indicator that reflects the order of influence of each factor, which is calculated as the difference between the maximum and minimum values of the three levels. The most significant factor has the highest R value. In this manner, the optimal concrete mix could be determined. A variance analysis was

Table 1: Chemical composition of ordinary Portland cement and fly ash (%).

Type	SiO_2	Al_2O_3	Fe_2O_3	CaO	MgO	SO_3	K_2O	Na_2O	Ti_2O	P_2O_5
OPC	22.13	7.35	3.93	61.22	4.07	1.52	0.47	0.99	0.35	0.05
FA	53.30	29.68	5.60	8.07	1.45	1.14	1.54	—	—	—

Note. OPC: ordinary Portland cement; FA: fly ash.

Table 2: Physical properties of nano-$CaCO_3$.

Average particle size (nm)	Specific surface area (m^2/g)	$CaCO_3$ content (%)	pH value	Apparent density (g/L)
15–40	180	98.9	8.5–10.5	300

Table 3: Factors and levels.

Factor/level	1	2	3
A (W/C)	0.4	0.5	0.6
B (fly ash content/%)	15	20	25
C (nano-CaCO3 content/%)	1	2	3

Table 4: Design table for the orthogonal experiments.

No.	A	B (%)	C (%)
A0	0.5	0	0
A1	0.4 (1)	15 (1)	1 (1)
A2	0.4 (1)	20 (2)	2 (2)
A3	0.4 (1)	25 (3)	3 (3)
A4	0.5 (1)	15 (1)	2 (2)
A5	0.5 (2)	20 (2)	3 (3)
A6	0.5 (2)	25 (3)	1 (1)
A7	0.6 (3)	15 (1)	3 (3)
A8	0.6 (3)	20 (2)	1 (1)
A9	0.6 (3)	25 (3)	2 (2)

conducted to test the significance of the factors. Based on the variance analysis theory, the sum of squares (SS), degree of freedom (DF), mean square (MS), and F values were computed. The F value is a major pointer reflecting the significance of factors. For a certain factor, the significance can be evaluated by comparing the F value with predetermined significance criteria: $F_{0.01}(2, 8)$ and $F_{0.05}(2, 8)$. A factor F value $> F_{0.01}(2, 8)$ indicates a major impact; $F_{0.05}(2, 8) < F$ value $< F_{0.01}(2, 8)$ indicates a moderate impact; F value $< F_{0.05}(2, 8)$ indicates a minor impact. Thus, the optimal concrete mix can be confirmed.

2.4. Mechanical Properties and Durability Experiments. Based on the orthogonal experiments, tests of the mechanical properties and durability of the optimal concrete were conducted. Two reference concrete mixtures were prepared in order to examine the influence of both the fly ash and the nano-$CaCO_3$. The strength test method was the same as above. Evaluation of the concrete durability properties included chloride penetrability, carbonation resistance, and frost resistance, in accordance with GB/T 50082-2009 [29]. The rapid chloride migration (RCM) test was used to measure the chloride penetrability at 28 d. After the test, the specimens were split into halves and sprayed with 0.1 mol/L silver nitrate to measure the chloride penetration depth. Then, the chloride ion diffusion coefficient of the concrete was calculated. The carbonation tests were carried out at 3, 7, 14, and 28 d, and the carbonation depths were tested by spraying a 1% phenolphthalein alcohol solution on the surface of the reserved side, which was not sealed with paraffin wax. The freeze-thaw tests utilized the rapid freezing and thawing method. One freeze-thaw cycle lasted for 3.5 h, with the highest temperature in the center of (5 ± 2) °C and lowest temperature of (-18 ± 2) °C. In total, 175 freeze-thaw cycles were conducted.

2.5. Microstructure Analysis. After the strength tests at the age of 7 and 28 d, small size of 3 to 5 mm pieces was taken from the specimens. The hydration reaction was stopped by putting them into pure alcohol. Then their microstructures were observed by SEM method. Before observation, the samples were sprayed with gold to improve the conductivity and then placed in the sample chamber. The sample microstructures were observed with a JSM-7610F field emission scanning electron microscope.

3. Results and Discussion

3.1. Optimal Mix Proportion. The results of the mechanical properties tests are presented in Figure 1. Figures 1(a), 1(b), and 1(c) show that A1 had the highest compressive strengths at 3, 7, and 28 d: 30.65 MPa, 41.43 MPa, and 53.30 MPa, respectively. Based on the compressive strength results, the optimal concrete mix is $A_1B_1C_1$, which corresponds to level 1 for the W/C, fly ash, and nano-$CaCO_3$ contents. This is followed by A2, which has W/C at level 1, fly ash at level 2, and nano-$CaCO_3$ at level 2. For the flexural strength, as shown in Figure 1(d), the optimal concrete mixture is A2, with mix proportions of $A_1B_2C_2$.

The range analysis results for the K and R values based on the compressive strength are listed in Table 5. Based on the R values, the order of the factor importance is as follows: W/C, nano-$CaCO_3$, and fly ash. According to the K value, the optimal mix for the 3 d compressive strength is $A_1B_1C_2$. At 7 d, the R values occur in the order of A, C, B, and the optimal mix is $A_1B_1C_1$. At 28 d, the R value in Table 5 indicates that the most significant factor is W/C, followed by fly ash, and nano-$CaCO_3$ exerts less influence on the compressive strength. Based on the order of K value for each factor, the optimal mix is determined as $A_1B_2C_1$.

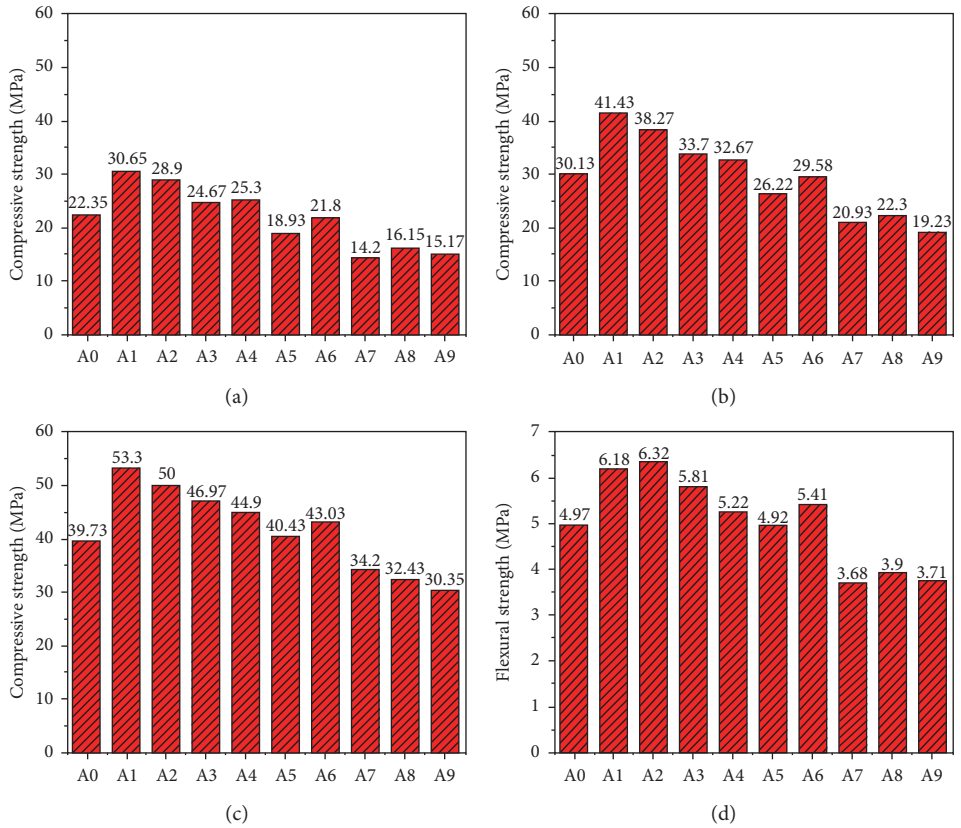

Figure 1: Results of the mechanical properties tests in the orthogonal experiments: compressive strengths at (a) 3 d, (b) 7 d, and (c) 28 d; (d) flexural strength at 28 d.

Table 5: Range analysis based on the compressive strength.

Level	3 d compressive strength			7 d compressive strength			28 d compressive strength		
	A	B	C	A	B	C	A	B	C
K_1	28.07	23.38	22.87	37.80	31.67	31.10	50.09	40.95	42.92
K_2	22.01	21.32	23.12	29.49	28.93	30.06	42.79	44.13	41.75
K_3	15.17	20.55	19.27	20.82	27.50	27.05	32.33	40.13	40.53
K	65.25	65.25	65.25	88.11	88.11	88.11	125.21	125.21	125.21
R	12.9	2.84	2.86	16.98	4.17	4.25	17.76	4.02	2.34

A variance analysis was also conducted based on the compressive strength, and the significance of factors was obtained; the results are listed in Table 6. The effect of W/C on the compressive strength is always significant. At 3 and 7 d, the influence of nano-$CaCO_3$ is greater than that of fly ash. The order of significance is A, C, B. At 28 d, nano-$CaCO_3$ does not have a significant effect on the compressive strength. The order of the factor importance is A, B, C. Thus, the range and variance analysis results are consistent.

Table 7 lists the results obtained from the range and variance analyses based on the flexural strength at 28 d. According to the K value, the optimal mix proportion is $A_1B_2C_1$. W/C has a significant effect on the concrete strength, while the other factors are not important. Thus, the range and variance analysis results are consistent, and the order of factor importance is A, C, B.

The optimal levels and the significance of factors obtained in the orthogonal analysis are summarized in Table 8; Figure 2 shows the effect of different levels on the mechanical properties. Thus, using the compressive strength and flexural strength as indices, the optimal levels for the concrete mixture could be determined.

As shown in Figure 2, curve A has the largest fluctuations, illustrating that W/C is the most significant factor affecting the performance of concrete. Therefore, the optimal level of W/C is determined as A_1 (0.4). For fly ash, the optimal level is B_1 at 3 and 7 d; however, Figure 2(c) indicates that the fly ash content is increased from B_1 to B_2 and the compressive strength at 28 d increased by 7.74%. With further increase in the fly ash content, curve B exhibits a downward trend. Considering that adding fly ash not only improves the concrete strength at later ages but also reduces the cost of concrete [30], the optimal level of fly ash was determined to be B_2 (20%). For nano-$CaCO_3$, the optimal level of C_1 is better than C_2 based on the visual analysis and range analysis. When the amount of nano-$CaCO_3$ increased

Table 6: Results of the variance analysis based on compressive strength.

Factors	3 d compressive strength				7 d compressive strength				28 d compressive strength			
	SS	DF	MS	F	SS	DF	MS	F	SS	DF	MS	F
A	249.9	2	125	664	432.6	2	216.3	570.3	478.3	2	239.1	232
B	12.9	2	6.4	32.2	27.0	2	13.5	35.0	27.0	2	13.5	13.1
C	27.9	2	11.0	74.1	28.0	2	14.0	36.9	8.6	2	4.3	4.1
Error	0.38	2	0.19	—	0.76	2	0.38	—	2.06	2	—	—
Total	291.1	8	—	—	488.3	8	—	—	515.8	8	—	—

Significance criteria: $F_{0.05}$ (2, 8) = 19; $F_{0.01}$ (2, 8) = 99.

Table 7: Range and variance analyses of the flexural strength.

Factors	K and R values					Sources of variation			
	$K1$	$K2$	$K3$	K	R	SS	DF	SD	F
A	6.10	5.18	3.76	15.04	2.34	8.34	2	4.17	222.36
B	5.02	5.05	4.97	15.04	0.07	0.01	2	0.01	0.21
C	5.16	5.08	4.80	15.04	0.36	0.21	2	0.11	5.71
Error	—	—	—	—	—	0.08	4	0.02	1.79
Total	—	—	—	—	—	8.63	8	—	—

Significance criteria: $F_{0.05}$ (2, 8) = 19; $F_{0.01}$ (2, 8) = 99.

Table 8: Comparison of the optimal mix proportions.

Index	Intuitive analysis	Range analysis	Factor order
3 d compressive strength	$A_1B_1C_1$	$A_1B_1C_2$	A > C > B
7 d compressive strength	$A_1B_1C_1$	$A_1B_1C_1$	A > C > B
28 d compressive strength	$A_1B_1C_1$	$A_1B_2C_1$	A > B > C
28 d flexural strength	$A_1B_2C_2$	$A_1B_2C_1$	A > C > B

from C_1 to C_2, the compressive strength at 3 d increased by 1.6%. However, it should be noted that when a high amount of nano-$CaCO_3$ is added to the concrete, the agglomeration of nano-$CaCO_3$, increase in viscosity, and reduction in flowability of the mixture can result in more cracks and air voids. Such cracks and air voids are triggers for the failure of concrete as they can have detrimental effects on the mechanical properties of concrete. The results indicate that, with an increase in the nano-$CaCO_3$ content from C_2 to C_3, the compressive strength at 28 d decreased by 16.65%. Moreover, the flexural strength exhibited the same trend at 28 d. In addition, considering the economic effect, C_1 is the optimal level for improving the concrete strength. Based on the above discussion, the optimal mix proportion is $A_1B_2C_1$, which represents a W/C of 0.4, 20% fly ash, and 1% nano-$CaCO_3$.

3.2. Effects of Nano-$CaCO_3$ and Fly Ash on the Mechanical Properties of Concrete. The mechanical properties of different concrete compositions are presented in Figure 3. The results show the effects of nano-$CaCO_3$ and fly ash on the strength of concrete. It is clear that sample NC (concrete with 20% fly ash and 1% nano-$CaCO_3$) had a higher strength than samples JZ (concrete without fly ash or nano-$CaCO_3$) and FA (concrete with 20% fly ash only) at all ages. As expected, on comparing JZ and FA, it can be observed that the compressive strength of the concrete with fly ash slowly increased at early ages but significantly improved at 28 d. Compared with FA, the compressive strength of NC was increased by approximately 10.98% and 12.98% at 3 and 7 d, respectively. However, this improvement ceased at 28 d, indicating that the addition of nano-$CaCO_3$ can compensate for the low compressive strength of concrete with fly ash at early ages but is quite limited at later ages; compared with JZ, NC exhibited higher compressive strengths at 3, 7, and 28 d, representing improvements of approximately 8.25%, 11.01%, and 13.67%, respectively. The results reveal that the combination of nano-$CaCO_3$ and fly ash in concrete is beneficial for improving the compressive strength.

As shown in Figure 3(b), the flexural strength of NC was increased by 19.00% and 8.22%, compared to JZ and FA, respectively, indicating that the addition of nano-$CaCO_3$ could increase the flexural strength of concrete, while the synergistic effect is much better than single-doped nano-$CaCO_3$.

3.3. Effects of Nano-$CaCO_3$ and Fly Ash on the Durability of Concrete. In Figure 4(a), it can be seen that the chloride diffusion coefficient of concrete JZ was the highest, representing the worst chloride resistance of the concrete samples. Compared with JZ, the chloride diffusion coefficients of FA and NC were decreased by 27.42% and 40.12%, respectively, indicating that fly ash can effectively limit the diffusion of chloride ions in concrete; the chloride resistance was further enhanced by the addition of 1% nano-$CaCO_3$. Previous studies [31, 32] have shown that the continuous evaporation

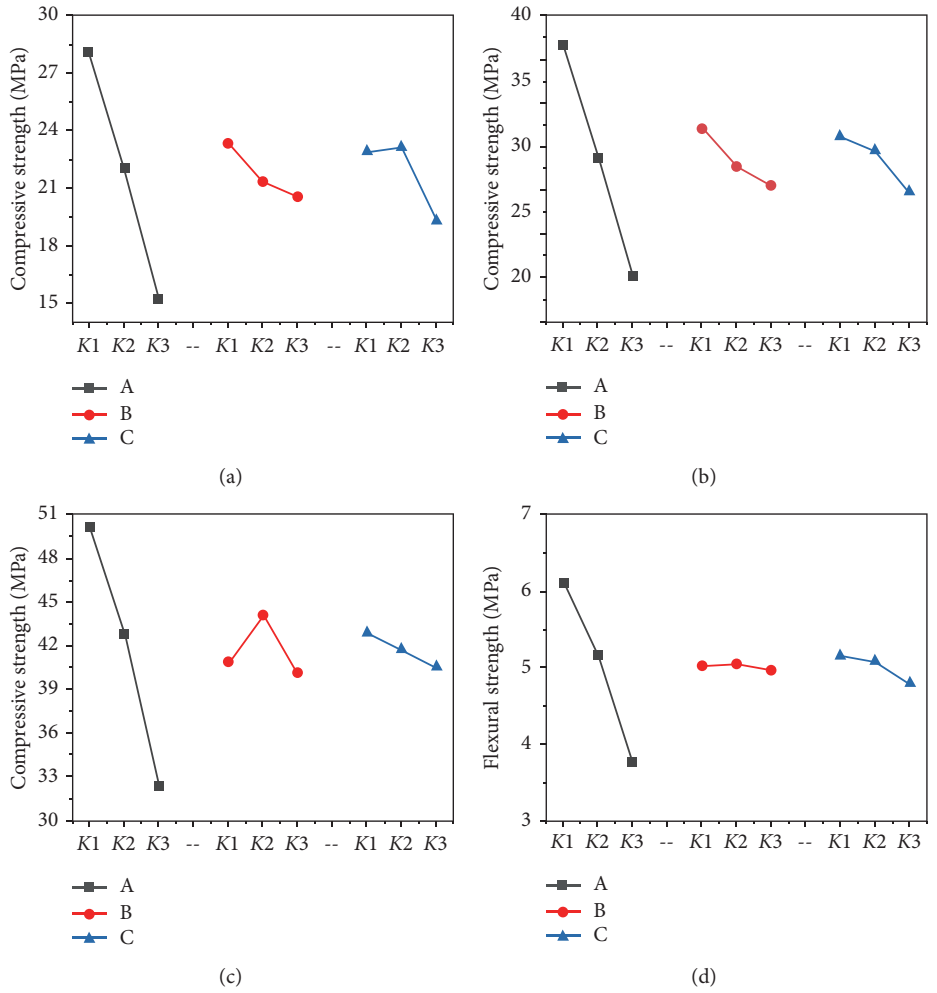

Figure 2: Impact of different levels: compressive strength at (a) 3 d, (b) 7 d, and (c) 28 d; (d) flexural strength at 28 d.

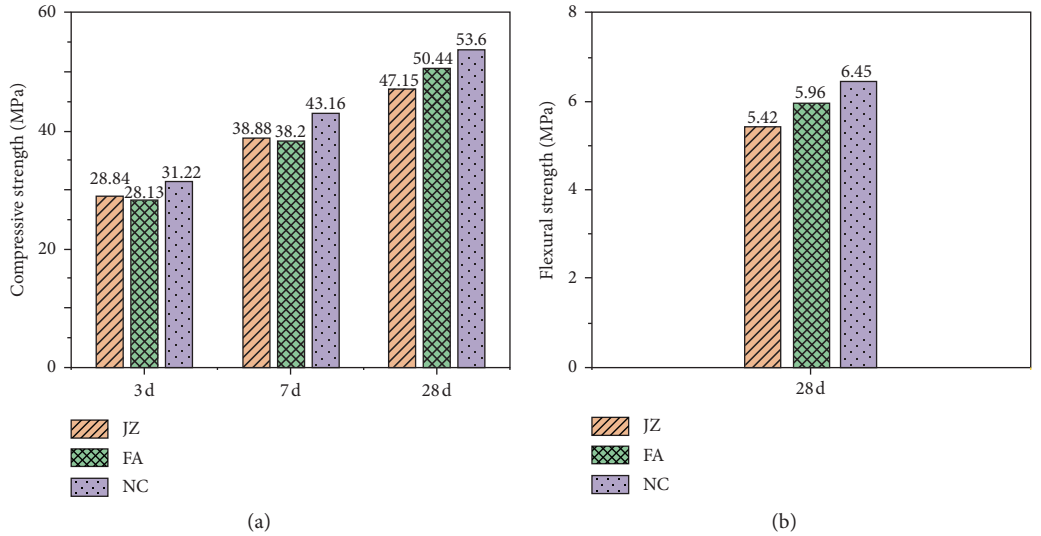

Figure 3: Mechanical properties of different concretes: (a) compressive strength at 3, 7, and 28 d; (b) flexural strength at 28 d.

of free water in the concrete during the hydration process caused a large number of pores to be left in the interior. These pores intersect with each other to form an open capillary bleeding channel, which increases the permeability. Only pore sizes larger than 50 nm will affect the permeability of concrete [33]. The filling effects of the fly ash can fill the

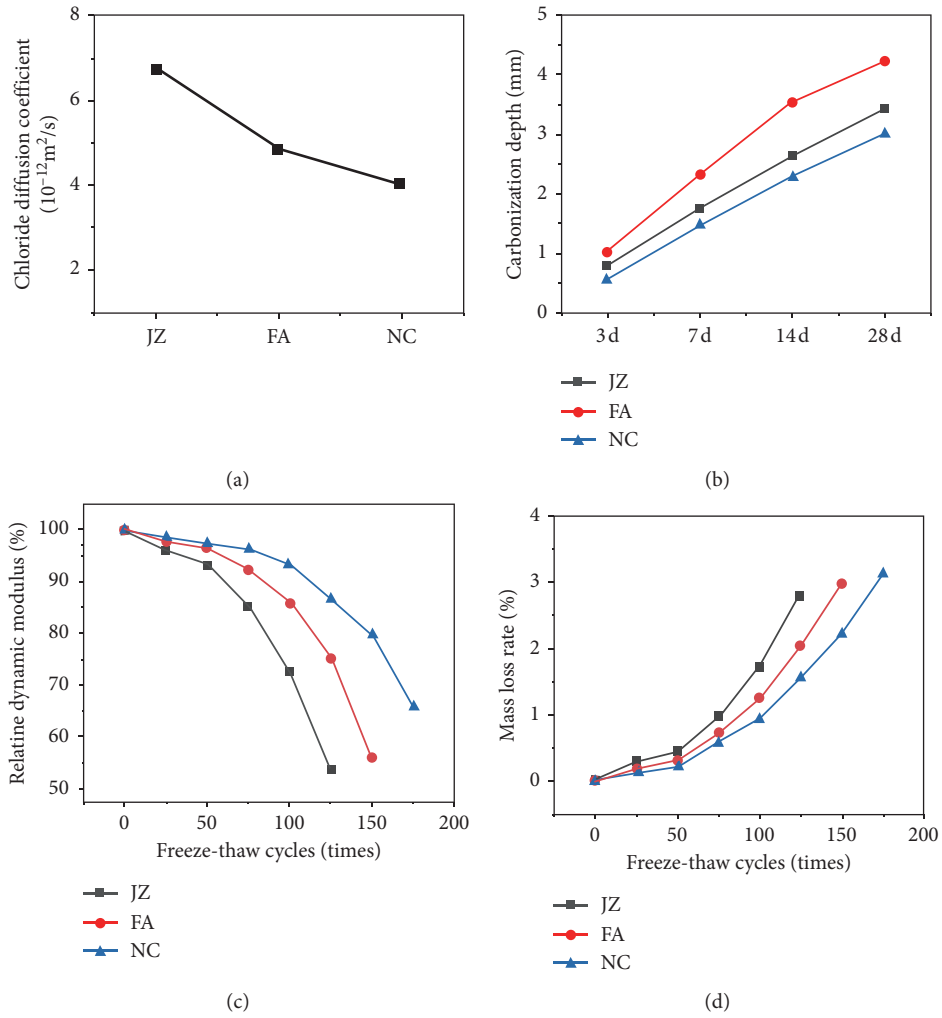

Figure 4: The results of durability tests: (a) chloride diffusion coefficient; (b) carbonation depth; (c) relative dynamic modulus; (d) mass loss rate.

tiny pores, and adding nano-CaCO3 can further refine the pore structure, transform the harmful pores into harmless or less pores, and reduce porosity. Therefore, nano-$CaCO_3$ and fly ash can significantly improve the permeability of concrete.

As shown in Figure 4(b), the concrete carbonation depth exhibited roughly the same trend of gradually deepening with age; the carbonation depth increased faster in the early stage than the later stage. This may be because $CaCO_3$ and other solid substances generated during the early carbonation of concrete blocked the internal micropores, thus reducing the diffusion rate of CO_2 [34]. The carbonation depth of FA is the largest, indicating that FA is more susceptible to carbonization. The reason is that fly ash can cause a "secondary reaction" with the cement hydration product $Ca(OH)_2$, which reduces the alkalinity of the pore solution and carbonizable substances, leading to a decreased resistance to carbonation [35, 36]. Comparing NC and FA shows that the addition of nano-$CaCO_3$ can not only make up for the adverse effect of fly ash but also greatly enhance the carbonation resistance.

As shown in Figures 4(c) and 4(d), before 50 freeze-thaw cycles, the relative dynamic elastic modulus of decay was slow, and the mass loss rate increased gradually. It is speculated that the loss process of concrete depends on the pore structure during the freeze-thaw process [37]. During the initial freezing and thawing of concrete, the degree of internal pore expansion is small. With an increasing number of freeze-thaw cycles, the tensile and compressive stresses generated in the concrete constantly change during the freezing and thawing processes, causing the internal pores to continuously expand, eventually forming cracks [38]. As a result, the rate of decrease in the relative dynamic elastic modulus of concrete accelerated continuously. Moreover, JZ exhibited a sharp mass loss when the number of freeze-thaw cycles reached 25, which represents the initiation of damage to the concrete; NC exhibited a much slower weight loss than JC. When the number of freeze-thaw cycles reached 175, the relative dynamic elastic modulus of NC was 65.79%, representing a decrease of 49.48%, and the mass loss rate was within 5%; JZ and FA were damaged after 125 and 150 freeze-thaw cycles, respectively. Compared to JZ, it can be

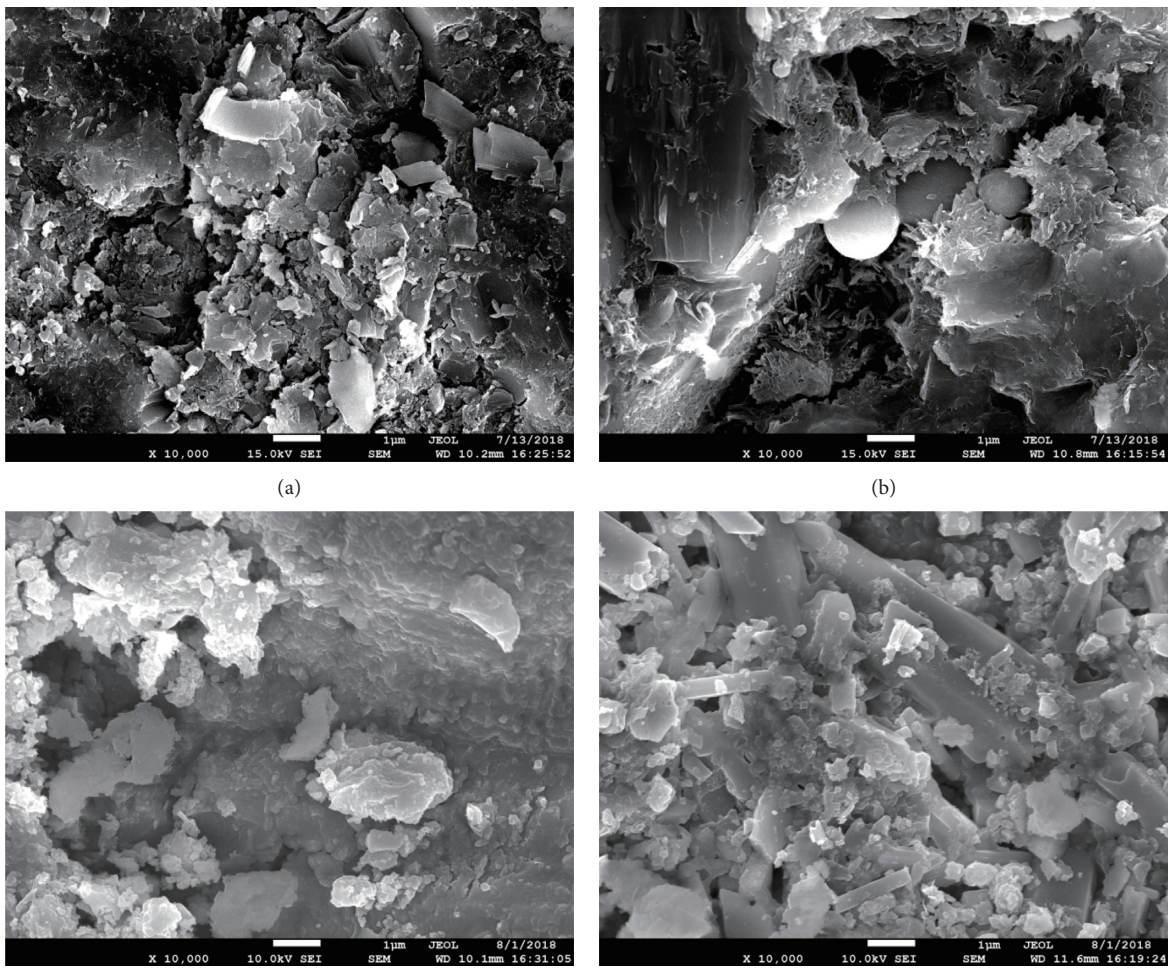

Figure 5: SEM images of different concretes: (a) JZ at 7 d; (b) NC at 7 d; (c) JZ at 28 d; (d) NC at 28 d.

seen that the frost resistance of NC has been greatly improved, indicating that the effect of combining nano-$CaCO_3$ and fly ash is beneficial for the frost resistance.

3.4. Effects of Nano-$CaCO_3$ and Fly Ash on the Microstructure of Concrete. Figure 5 shows SEM images of selected concrete samples JZ and NC at 7 and 28 d, respectively. Comparing Figures 5(a) and 5(b) shows that the microstructure of sample JZ was relatively loose, confirming that the degree of hydration of JZ was lower than that of NC. As shown in Figure 5(a), many hydration products were formed on the surface of the fly ash particles, and it appears that a network-type structure was formed by these hydrates as a result of the accelerated hydration of cement and fly ash by nano-$CaCO_3$. Furthermore, some small piles, which may be composed of nano-$CaCO_3$, hydrates, and fly ash, can be observed in the network. This may also indicate nano-$CaCO_3$ was helpful for accelerating the hydration process as a result of its high hydration activity and ability to provide nucleation sites. In addition, researchers have found [39] that nano-$CaCO_3$ can increase the content of C-S-H gel at the interface and improve the orientation of Ca $(OH)_2$ crystals, resulting in a transition in the hydration structure at the interface position from a planar arrangement to a spatial structure. Moreover, nano-$CaCO_3$ filled up the pores of loose net structure around the cement particles, thereby decreasing the porosity of concrete and increasing the density degree [40]. Thus, it can be concluded that nano-$CaCO_3$ was helpful for increasing the hydration degree and enhancing the strength of concrete at early ages.

With continued progress of the hydration, the microstructure became more compact at 28 d, as shown in Figures 5(c) and 5(d). A comparison of (c) and (d) reveals that, with the generation of new C-S-H gels and the growth of ettringite crystals, the internal pores in the cement became more completely filled. After 28 d, the C-S-H gels and ettringites attached to each other and needle-like ettringites were wrapped by the C-S-H gels, which also contributed to increasing the density. This may be a result of the pozzolanic effect of the fly ash, which plays an important role in the improvement of strength at later ages.

Based on the above analysis, it can be concluded that concrete containing nano-$CaCO_3$ and fly ash can accelerate the hydration process and lead to a denser microstructure, consequently enhancing the mechanical properties and

durability of the concrete. This may be the result of a few mechanisms: the seeding effect, filling effect, and pozzolanic effect.

4. Conclusions

Based on the results of this study, the following conclusions can be drawn:

(1) An evaluation revealed that the concrete with a W/C ratio of 0.4, 20% fly ash, and 1% nano-$CaCO_3$ exhibited the best mechanical properties.

(2) Under the synergistic effect of nano-$CaCO_3$ and fly ash, the durability of the concrete was significantly enhanced owing to the filling effect. In particular, with the addition of nano-$CaCO_3$, the adverse effects of fly ash on the carbonation resistance could be balanced out.

(3) SEM analysis reveals that nano-$CaCO_3$ was helpful for increasing the compressive strength of the concrete at early ages due to the acceleration of cement hydration by the seeding effect and the tighter pore structure of cement as a result of nanofilling. On the other hand, the pozzolanic effect of the fly ash at later ages can further enhance the mechanical strength of concrete, making up for the limited effect of the nano-$CaCO_3$.

For practical applications, reasonable guidance on the optimal concrete mix proportion can be provided. However, detailed researches on the production and preparation technology of nanomaterials are required to facilitate the application of nanomodified concrete.

Data Availability

All the data used to support the findings of this study are included within the article.

Conflicts of Interest

The authors declare no conflicts of interest.

Acknowledgments

Financial support for ongoing projects from the National Natural Science Foundation of China (51922052, U1706222, and 51778309) and the Natural Science Foundation of Shandong Province (ZR2018JL018) is gratefully acknowledged.

References

[1] F. Pacheco-Torgal and S. Jalali, "Nanotechnology: advantages and drawbacks in the field of construction and building materials," *Construction and Building Materials*, vol. 25, no. 2, pp. 582–590, 2011.

[2] M. F. Najjar, M. L. Nehdi, A. M. Soliman, and T. M. Azabi, "Damage mechanisms of two-stage concrete exposed to chemical and physical sulfate attack," *Construction and Building Materials*, vol. 137, no. 4, pp. 141–152, 2017.

[3] D. Wang, X. Zhou, Y. Meng, and Z. Chen, "Durability of concrete containing fly ash and silica fume against combined freezing-thawing and sulfate attack," *Construction and Building Materials*, vol. 147, no. 8, pp. 398–406, 2017.

[4] M. S. Kirgiz, "Advance treatment by nanographite for Portland pulverised fly ash cement (the class *F*) systems," *Composites Part B: Engineering*, vol. 82, no. 12, pp. 59–71, 2015.

[5] P. Zhang, D. Li, Y. Qiao, S. Zhang, C. Sun, and T. J. Zhao, "The effect of air entrainment on the mechanical properties, chloride migration and microstructure of ordinary concrete and fly ash concrete," *Journal of Materials in Civil Engineering*, vol. 30, no. 10, Article ID 04018265, 2018.

[6] S. B. Xue, P. Zhang, J. W. Bao, L. F. He, Y. Hu, and S. D. Yang, "Comparison of mercury intrusion porosimetry and multiscale X-ray CT on characterizing the microstructure of heat-treated cement mortar," *Materials Characterization*, vol. 160, no. 2, Article ID 110085, 2020.

[7] J. W. Bao, S. G. Li, P. Zhang et al., "Influence of the incorporation of recycled coarse aggregate on water absorption and chloride penetration into concrete," *Construction and Building Materials*, vol. 239, no. 4, Article ID 117845, 2020.

[8] Y. Su, J. Li, C. Wu, P. Wu, and Z.-X. Li, "Influences of nanoparticles on dynamic strength of ultra-high performance concrete," *Composites Part B: Engineering*, vol. 91, no. 4, pp. 595–609, 2016.

[9] M.-H. Zhang and J. Islam, "Use of nano-silica to reduce setting time and increase early strength of concretes with high volumes of fly ash or slag," *Construction and Building Materials*, vol. 29, no. 4, pp. 573–580, 2012.

[10] A. Nazari and S. Riahi, "The effects of SiO_2 nanoparticles on physical and mechanical properties of high strength compacting concrete," *Composites Part B: Engineering*, vol. 42, no. 3, pp. 570–578, 2011.

[11] B.-W. Jo, C.-H. Kim, G.-H. Tae, and J.-B. Park, "Characteristics of cement mortar with nano-SiO_2 particles," *Construction and Building Materials*, vol. 21, no. 6, pp. 1351–1355, 2007.

[12] A. Nazari, R. Shadi, R. Shirin, S. F. Shamekhi, and A. Khademno, "Mechanical properties of cement mortar with Al_2O_3 nanoparticles," *Journal of American Science*, vol. 6, no. 4, pp. 94–97, 2010.

[13] L. Senff, J. A. Labrincha, V. M. Ferreira, D. Hotza, and W. L. Repette, "Effect of nano-silica on rheology and fresh properties of cement pastes and mortars," *Construction and Building Materials*, vol. 23, no. 7, pp. 2487–2491, 2009.

[14] A. Nazari, R. Shadi, R. Shirin, S. F. Shamekhi, and A. Khademno, "Influence of Al_2O_3 nanoparticles on the compressive strength and workability of blended concrete," *Journal of American Science*, vol. 6, no. 5, pp. 6–9, 2010.

[15] E. García-Taengua, M. Sonebi, K. M. A. Hossain, M. Lachemi, and J. Khatib, "Effects of the addition of nanosilica on the rheology, hydration and development of the compressive strength of cement mortars," *Composites Part B: Engineering*, vol. 81, no. 11, pp. 120–129, 2015.

[16] T. Sato and J. J. Beaudoin, "Effect of nano-$CaCO_3$ on hydration of cement containing supplementary cementitious materials," *Advances in Cement Research*, vol. 23, no. 1, pp. 1–29, 2010.

[17] P. Hou, K. Wang, J. Qian, S. Kawashima, D. Kong, and S. P. Shah, "Effects of colloidal nano SiO_2 on fly ash hydration," *Cement and Concrete Composites*, vol. 34, no. 10, pp. 1095–1103, 2012.

[18] F. Sanchez and K. Sobolev, "Nanotechnology in concrete—a review," *Construction and Building Materials*, vol. 24, no. 11, pp. 2060–2071, 2010.

[19] G. Kakali, S. Tsivilis, E. Aggeli, and M. Bati, "Hydration products of C_3A, C_3S and Portland cement in the presence of $CaCO_3$," *Cement and Concrete Research*, vol. 30, no. 7, pp. 1073–1077, 2000.

[20] T. Meng, Y. Yu, and Z. Wang, "Effect of nano-$CaCO_3$ slurry on the mechanical properties and micro-structure of concrete with and without fly ash," *Composites Part B: Engineering*, vol. 117, no. 5, pp. 124–129, 2017.

[21] T. Meng, K. Qian, X. Qian, and S. Zhan, "Effect of the nano-$CaCO_3$ on hydrated properties and interface of cement paste," *Rare Metal Materials and Engineering*, vol. 37, no. 5, pp. 667–669, 2008.

[22] T. Sato and F. Diallo, "Seeding effect of nano-$CaCO_3$ on the hydration of tricalcium silicate," *Transportation Research Record: Journal of the Transportation Research Board*, vol. 2141, no. 1, pp. 61–67, 2010.

[23] S. W. M. Supit and F. U. A. Shaikh, "Effect of nano-$CaCO_3$ on compressive strength development of high volume fly ash mortars and concretes," *Journal of Advanced Concrete Technology*, vol. 12, no. 6, pp. 178–186, 2014.

[24] Q. L. Xu, T. Meng, and M. Z. Huang, "Effects of nano-$CaCO_3$ on the compressive strength and microstructure of high strength concrete in different curing temperature," *Applied Mechanics and Materials*, vol. 121–126, no. 1, pp. 126–131, 2011.

[25] Z. Ge, Z. Gao, R. Sun, and L. Zheng, "Mix design of concrete with recycled clay-brick-powder using the orthogonal design method," *Construction and Building Materials*, vol. 31, no. 7, pp. 289–293, 2012.

[26] C. Standard, GB/T50081-2002.

[27] M. Stefanidou and I. Papayianni, "Influence of nano-SiO_2 on the Portland cement pastes," *Composites Part B: Engineering*, vol. 43, no. 6, pp. 2706–2710, 2012.

[28] S. C. K. Bendapudi and P. Saha, "Contribution of fly ash to the properties of mortar and concrete," *International Journal of Earth Sciences and Engineering*, vol. 4, no. 6, pp. 1017–1023, 2011.

[29] C. Standard, GB/T50082-2009.

[30] G. Land and D. Stephan, "The influence of nano-silica on the hydration of ordinary Portland cement," *Journal of Materials Science*, vol. 47, no. 2, pp. 1011–1017, 2012.

[31] Y. Wang, Y. Cao, P. Zhang et al., "Water absorption and chloride diffusivity of concrete under the coupling effect of uniaxial compressive load and freeze-thaw cycles," *Construction and Building Materials*, vol. 209, no. 6, pp. 566–576, 2019.

[32] F. U. A. Shaikh and S. W. M. Supit, "Chloride induced corrosion durability of high volume fly ash concretes containing nano particles," *Construction and Building Materials*, vol. 99, no. 11, pp. 208–225, 2015.

[33] T. Gonen and S. Yazicioglu, "The influence of compaction pores on sorptivity and carbonation of concrete," *Construction and Building Materials*, vol. 21, no. 5, pp. 1040–1045, 2007.

[34] S. Kawashima, P. Hou, D. J. Corr, and S. P. Shah, "Modification of cement-based materials with nanoparticles," *Cement and Concrete Composites*, vol. 36, no. 5, pp. 8–15, 2013.

[35] J. Camiletti, A. M. Soliman, and M. L. Nehdi, "Effects of nano- and micro-limestone addition on early-age properties of ultra-high-performance concrete," *Materials and Structures*, vol. 46, no. 6, pp. 881–898, 2013.

[36] S. A. Barbhuiya, J. K. Gbagbo, M. I. Russell, and P. A. M. Basheer, "Properties of fly ash concrete modified with hydrated lime and silica fume," *Construction and Building Materials*, vol. 20, no. 3, pp. 3233–3239, 2009.

[37] P. Zhang, F. H. Wittmann, M. Vogel, H. S. Müller, and T. Zhao, "Influence of freeze-thaw cycles on capillary absorption and chloride penetration into concrete," *Cement and Concrete Research*, vol. 100, no. 10, pp. 60–67, 2017.

[38] J. Bao, S. Xue, P. Zhang, Z. Dai, and Y. Cui, "Coupled effects of sustained compressive loading and freeze-thaw cycles on water penetration into concrete," *Structural Concrete*, vol. 1–11, 2020.

[39] A. Chaipanich, T. Nochaya, W. Wongkeo, and P. Torkittikul, "Compressive strength and microstructure of carbon nanotubes-fly ash cement composites," *Materials Science and Engineering: A*, vol. 527, no. 1, pp. 1063–1076, 2010.

[40] H. Li, H.-G. Xiao, J. Yuan, and J. Ou, "Microstructure of cement mortar with nano-particles," *Composites Part B: Engineering*, vol. 35, no. 2, pp. 185–189, 2004.